

Design of a system to measure light scattering from individual cells excited by an acoustic wave

Ramona Georgescu¹, Damir Khismatullin², R. Glynn Holt³, Jean Luc Castagner²,
Ousama A'amar² and Irving J. Bigio^{1, 2 *}

¹Boston University, Dept. of Electrical & Computer Engineering, Boston, MA 02215

²Boston University, Dept. of Biomedical Engineering, Boston, MA 02215

³Boston University, Dept. of Aerospace & Mechanical Engineering, Boston, MA 02215

*Corresponding author: bigio@bu.edu

Abstract: A system to measure light scattering from individual cells excited by an acoustic wave was designed, and tests were performed on live Jurkat cells. Cells passing in a laminar stream within a water bath were excited by a focused ultrasound pulse, while the scattered light from a laser beam was monitored at various scattering angles. The cells were modeled as viscoelastic liquid drops, which return to equilibrium via shape oscillations after an acoustically-induced deformation. The Fast Fourier Transform of the scattered light signal was used to extract information about the highly-damped resonant frequencies of the cells, and the detected frequencies are consistent with theoretical predictions.

© 2008 Optical Society of America

OCIS codes: (170.1065) Acousto-optics; (170.1530) Cell analysis; (290.4020) Mie theory

References and links

1. J. D. Keener, K. J. Chalut, J. W. Pytila, and A. Wax, "Application of Mie theory to determine the structure of spheroidal scatterers in biological materials," *Opt. Lett.* **32**, 1326-1328 (2007).
2. F. Xu, K. Ren, G. Gouesbet, G. Gréhan, and X. Cai, "Generalized Lorenz-Mie theory for an arbitrarily oriented, located, and shaped beam scattered by a homogeneous spheroid," *J. Opt. Soc. Am. A* **24**, 119-131 (2007).
3. G. M. Cooper and R. E. Hausman, *The Cell: A Molecular Approach*, (ASM Press, 2003).
4. R. Piga, R. Micheletto, and Y. Kawakami, "Acoustical nanometre-scale vibrations of live cells detected by a near-field optical setup," *Opt. Express* **15**, 5589-5594 (2007).
5. J. Novy, P. Becvarova, J. Skorpikova, V. Mornstein and R. Janisch, "Discrete Fourier Transform-based analysis of HeLa cell microtubules after ultrasonic exposure," *Microsc. Res. Tech.* **68**, 1-5 (2005).
6. S. H. Bloch, R. E. Short, K. W. Ferrara, and E. R. Wisner, "The effect of size on the acoustic response of polymer-shelled contrast agents," *Ultrasound Med. Biol.* **31**, 439-444 (2005).
7. M. S. Roos and R. E. Apfel, "Application of 30-MHz acoustic scattering to the study of human red blood cells," *J. Acoust. Soc. Am.* **83**, 1639-1644 (1988).
8. L. Haider, P. Snabre and M. Boynard, "Rheology and Ultrasound Scattering from Aggregated Red Cell Suspensions in Shear Flow," *Biophysics J.* **87**, 2322-2334, 2004.
9. C. Bohren and D. R. Huffman, *Absorption and Scattering of Light by Small Particles*, (Wylie, 1998).
10. C.S. Mulvey, A.L. Curtis, S.K. Singh and I.J. Bigio, "Elastic scattering spectroscopy as a diagnostic tool for apoptosis in cell cultures," *IEEE J. Sel. Topics in Quantum Electron.* **13**, 1663-1670 (2007).
11. H. C. Van de Hulst, *Light Scattering by Small Particles*, (Wylie, 1957).
12. R. A. Roy and R. E. Apfel, "Mechanical characterization of microparticles by scattered ultrasound," *J. Acoust. Soc. Am.* **87**, 2332-2341 (1990).
13. G. Chen, N. Chen, A. L. Garner, J. Kolb, R. J. Swanson, S. Beebe, R. P. Joshi and K. H. Schoenbach, "Conductivity in Jurkat cell suspensions after ultrashort electric pulsing," *Proc. 3rd Int'l. Workshop on Biological Effect of EMFs*, 56-65 (2004).
14. D. B. Khismatullin and A. Nadim, "Shape oscillations of a viscoelastic drop," *Phys. Rev. E* **63**, 061508 (2001).
15. C. Dong and X. Lei, "Biomechanics of cell rolling: Shear flow, cell-surface adhesion, and cell deformability," *J. Biomech.*, **33**, 35-43 (2000).
16. D. B. Khismatullin and G. A. Truskey, "Three-dimensional numerical simulation of receptor-mediated leukocyte adhesion to surfaces: Effects of cell deformability and viscoelasticity," *Phys. Fluids* **17**, 031505 (2005).
17. C. A. Miller and L. E. Scriven, "The oscillations of a fluid droplet immersed in another fluid," *J. Fluid Mech.* **32**, 417-435 (1968).

18. E. D. Hirtleman, "Laser-based single particle counters for in situ particulate diagnostics," *Opt. Eng.* **19**, 854-860 (1980).
 19. D. Holve and S. A. Self, "Optical particle sizing for in situ measurements-Part 1," *Appl. Opt.* **18**, 1632-1645 (1979).
-

1. Introduction

The motivation for this project is to develop a hybrid optical/acoustical method to provide information about the mechanical and rheological properties of individual cells. In particular, our ultimate goal is to better understand the cytoskeleton and mechanical/morphological changes associated with a cell's progression towards a diseased state. For the work reported here our initial goal was to demonstrate that light scattering from cells can sense motion/oscillations induced by an acoustic wave. It is our expectation that our technique would be ultimately quantitative, and it is designed to be noninvasive, inexpensive and to provide real-time evaluation of individual viable cells. The work described in this report is the first-stage, proof-of-concept, of this research. It describes our efforts at detecting changes in the scattered light intensity from cells, due to shape oscillations induced by an acoustical pulse. Generalized Lorentz-Mie theory predicts that the scattering efficiency will depend on shape, and therefore will vary with shape oscillations. [1, 2]

One of the parameters that govern a cell's shape and mechanical properties is the cytoskeleton. The cytoskeleton is a network of protein filaments extending throughout the cytoplasm, which determine cell shape, and the positions of the nucleus and other organelles. It is a dynamic structure; e.g., the intermediate filaments can increase in density in response to mechanical stress. [3]

Piga, *et al.*, (2005) made one of the few attempts to look at the cytoskeleton quantitatively. [4] With a scanning near-field optical microscope (SNOM) they were able to detect tiny and sudden vertical vibrations on the membrane (1-10nm) of undifferentiated PC12 cells, which could be associated with the physiological activity of the cell, such as dynamics of the cytoskeletal system and/or cyclic duplication and division. [5]

There have been a few reports of methods to study the mechanical properties of cells at acoustic frequencies. Bloch, *et al.*, developed a setup that uses ultrasound for both excitation and detection to investigate the effect of size on the acoustic response of polymer shelled contrast agents. [6] Red blood cells subjected to acoustic scattering have been used in studies of cell mechanics and cell rheology. [7, 8]

Our setup is based on concepts from flow cytometry, but with the addition of an ultrasound beam that is focused on the same spot as a laser beam. The role of the ultrasound is to induce acoustic-frequency mechanical deformations of the cells, which are detected optically with scattered light. An instrument for angular light scattering measurements is often called a polar nephelometer. In simplest form, its essential elements are a collimated light source and an arm with a detector that can be rotated about the sample (a goniometer arrangement). The detector includes optical elements to collect light scattered within a small solid angle.

To successfully obtain angular light scattering information from single particles, it is usually necessary to take one of two approaches: stably suspend the particles and use a conventional nephelometer, or make more rapid measurements on individual particles in flow. Scattering data can be recorded rapidly in the short time it takes a particle to transit the test space. This can be done in two ways: with a rotating detector arm or with an array of fixed detectors. [9] Systems that are not automated usually suffer from lengthy testing times. Our instrument analyzes particles in flow with a rotating detector that was not yet automated during these proof-of-concept measurements.

Photons scatter elastically from gradients and discontinuities in the optical refractive index of cells and sub-cellular structures. The scattering that occurs depends on multiple parameters: the size, shape and index of refraction of the scatterer, the index of refraction of the medium, the wavelength and polarization of the incident light, and the detection angle. By measuring the wavelength dependence and/or the angular dependence of light scattered

from cells, elastic scattering spectroscopy (ESS) can infer information about the structural properties. Since pathologists use these morphological features of cells to diagnose disease, ESS has been demonstrated to be a promising diagnostic tool. [9-11]

A benefit to using light scattering to probe cell morphology is its noninvasiveness, as contact with the cell is not required. Another benefit of ESS is that measurements can be taken without fixation or the use of stains or other exogenous agents, which disrupt cell viability. ESS measurements can be made quickly, usually within milliseconds. With proper analysis algorithms, cellular state can be determined in real time. Finally, depending on the setup, experiments can be performed on a number of cells to obtain an average population measurement, or can be made on a single cell to determine population statistics. [10]

2. Experimental methods

Our setup is based on an extrapolation of one developed by Roy, *et al.*, [12]. Using a focused ultrasound transducer as an excitation source and a transducer as a detector, they calculated, based on ultrasound scattering theory, the compressibility and density of a particle given that its size and the host fluid properties were known *a priori*.

The system for our experiments is depicted in Figs. 1 and 2. A syringe pump (Kent Scientific Genie Plus) pushes a dilute suspension of cells through a 30-gauge needle, whose tip is submerged in a water bath. At the exit, the needle is encased by a glass nozzle (3mm i.d.), which ensures a laminar flow at the exit of the nozzle. The needle passes through a T-connector, and a reservoir provides filtered (0.2 μ m) water to the side entry port of the T-connector. In the nozzle, the particle suspension is further diluted by mixing with the filtered water, so that at the system can perform light scattering measurements on one particle at a time. The assembly is affixed on an xyz-positioner to facilitate the accurate placement of the jet flow with respect to the acoustic and optical beams. The nozzle and jet flow are all submerged in a water bath, which provides conductance of the acoustic wave. A "sink" in the bath, underneath the nozzle, collects the jet downstream and transfers it to a waste reservoir by controlled gravity flow. The result is laminar flow for the stream of cells, and the velocity of the cells in the focal zone is ~ 1 m/sec.

A focused ultrasound (US) transducer is the acoustic excitation source, but rather than detecting the scattered US signal, an optical system was implemented to detect changes in light scattering induced by the US wave. The US source used in the experiments is a single-element, spherically focused transducer (Sonic Concepts SU-109) with a center frequency of 6.8 MHz, a Q of approximately 1, a geometrical focus of 35 mm and an f-number of 1.5. The estimated focal dimensions for the main lobe are 0.75mm radial by 7mm axial. The transducer is impulse excited by a driver/receiver card, with short electrical pulses (50 nsec) at a pulse repetition rate of 10kHz. This induces broadened US pulses from the transducer, lasting only a few cycles, centered at 6.8 MHz but broadband, which stimulate cells with a wide range of frequencies. The amplitude of the electrical drive pulse was set low enough to avoid cavitation in the focal region. This was verified by the fact that there was no significant optical scattering from the focal zone in the absence of test particles or cells, whereas the presence of cavitation bubbles would have caused very strong optical scattering - much stronger than that from the cells themselves. A data acquisition card (National Instruments PCI6014), controlled with Labview, is used to provide the trigger for the driver/receiver card, and also digitizes the signal from the photodetector.

After being deformed by this mechanical stress induced by the US pulse, the cells return to equilibrium by highly-damped shape oscillations at a characteristic range of frequencies. Therefore, the center frequency of the transducer is not critical. The excitation transducer is mounted on an xyz-positioner for alignment purposes. A needle hydrophone (Dapco PZT) was used to align the acoustic focus with the laser focus after the alignment of the laser beam with the fluid jet was accomplished.

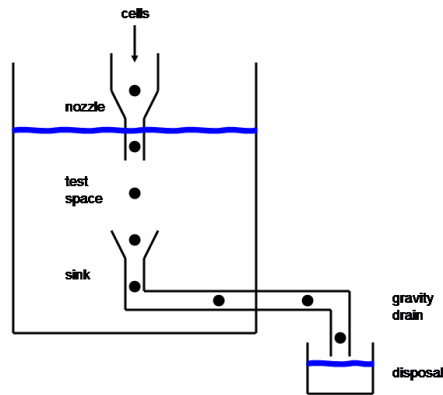


Fig. 1. Laminar flow setup.

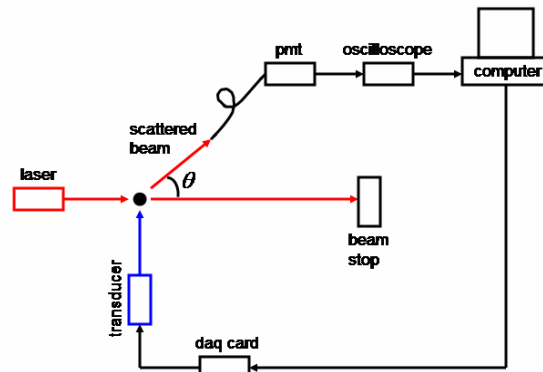


Fig. 2. Excitation-detection system.

An unpolarized 633nm HeNe laser (JDS Uniphase 1101) is weakly focused on the fluid jet at the same spot where the US transducer is focused, such that they both hit each cell approximately 1mm below the point where the particles exit the nozzle. The intersection of the confocal regions of the laser and the transducer is referred to as the test space. A submerged optical fiber (core diameter = 400 μ m) is mounted on a rotating arm, thereby being able to collect light at a range of angles, one angle at a time. A 1-mm diameter pinhole placed 2 cm in front of the fiber sets the angular resolution to less than 1 degree. The fiber sends the collected scattered light through an interference filter to a photomultiplier tube (PMT - Hamamatsu H8249-102). The PMT signal is recorded by a digital oscilloscope (Tektronix TDS3032) with sampling frequency 2.5GS/sec, which downloads to a computer via GPIB controlled by Matlab.

Calibration was performed with the ultrasound off using polystyrene microspheres (2.92 μ m diameter, Duke Scientific Corp.), which are routinely used for calibration of nephelometers due to the particles' narrow size distribution. Measurements were taken in 2-degree steps both in the forward and backscattering regimes, and results were consistent with Mie theory. However, polystyrene spheres are too rigid to be significantly deformed by the ultrasound pulses; thus, they cannot serve as a phantom for cells. For testing proof-of-concept, Jurkat cells were employed.

Jurkat cells (from ACCT) are a commonly studied cell line, easy to culture, grown in suspension and have an average nuclear diameter of 7-8 μ m [13], with a range of values published in the literature. The cells were grown in suspension in polystyrene culture flasks. The medium used was RPMI medium 1640, supplemented with 10% fetal bovine serum (FBS) and 1% penicillin and streptomycin (PAS). The cultures were initially seeded at a density of 3-5 $\times 10^5$ cells/ml. Subculturing occurred when the density reached about 2 $\times 10^6$ cells/ml, accomplished by adding fresh medium until concentration reached seeding density. Counting the cells was accomplished with a hemocytometer and 4% trypan blue. Before use in the experiment, the cells were resuspended in phosphate-buffered saline (PBS), which kept them viable for the short time between culturing and experiment. The flow medium was also PBS, and due to the laminar flow and the very short time (~1 msec) between exiting the nozzle and being measured, the cells were not exposed to the pure water of the main bath until after passing through the test space.

Optical scattering is strongest from the cell nucleus. Organelles generate less scattering; while the contribution to scattering by the cell membrane is very small and is generally not taken into account. In our study only the scattering by the nucleus was considered. The PBS has a slightly higher index of refraction than the pure water of the larger bath, and optical scattering from the interface of the laminar flow jet with the water bath was small and

constant compared with scattering from the cells. Thus, this low-level background was easy to subtract from the cell signals.

3. Analytical approach

A theoretical framework for shape oscillations of viscoelastic cells was developed by Khismatullin and Nadim [14]. We have applied the method to the nucleus, rather than the whole cell, because, as stated above, the ESS signal comes predominantly from the nucleus and (to a lesser extent) smaller organelles, whereas the whole-cell membrane is a very weak source of optical scattering. In this paper, normal mode analysis was performed to determine the effect of bulk viscoelasticity on resonant properties of drop shape oscillations in microgravity, i.e., under the conditions when the Bond number $B = gR^2(\rho_c - \rho_w)/\sigma$, which expresses the ratio of gravitational to surface tension forces, is much less than unity. Here, ρ_c is the density of the drop (the nucleus in our case), ρ_w the water density, R the drop radius, g the acceleration due to gravity, and σ the drop-water interfacial tension (cortical tension in our case).

In our experiments, the Bond number is very small because the nucleus density deviates insignificantly from the water density. Describing drop viscoelasticity by the linear Jeffreys constitutive equation, Khismatullin and Nadim [14] derived the characteristic equation for the natural frequency and decay factor of drop shape oscillations and discovered that the drop elasticity (specifically, the relaxation time λ_{1c}) gives rise to a type of shape oscillation that does not depend on the interfacial tension. This elasticity-driven shape oscillation occurs when the drop viscosity is high and the relaxation time is above a critical value. For small to moderate relaxation times, they found that the frequency of this oscillation ω_{el} is described by the following formula:

$$\omega_{el} = \sqrt{\frac{2(n-1)(2n^2+4n+3)\mu_c}{(2n+1)(1+E_n)\rho_c R^2 \lambda_{1c}}}, \quad E_n = \frac{4n(n-1)(n+2)}{(2n+1)(2n+3)(2n+5)}, \quad (1)$$

where n is the normal mode number and μ_c is the drop viscosity (cell viscosity in our case). The case of $n=2$ describes a quadrupole shape oscillation at which the nucleus shape alternates between a prolate and oblate spheroid [12]. Under the assumption that the nuclear radius is $R = 4\mu\text{m}$, density $\rho_c = 1040\text{ kg/m}^3$, viscosity $\mu_c = 5\text{ Pa}\cdot\text{s}$ [15], and relaxation time $\lambda_{1c} = 0.176\text{ s}$ [16], Eq. (1) predicts that the natural frequency of quadrupole shape oscillation of a Jurkat cell nucleus is $f_{el} = \omega_{el}/2\pi = 17.28\text{ kHz}$. It should be noted that ω_{el} is very sensitive to the particle radius. The nuclei of Jurkat cells used in our experiments do not have a narrow size distribution ($\sim 5\%$) and, therefore, we expect a range of natural frequencies in the scattering signal centered in the proximity of 17.28 kHz.

To ensure that Eq. (1) provides a good approximation to the natural frequency of viscoelastic shape oscillations in water, we solved numerically with Maple the general characteristic equation for drop oscillation in an aqueous medium (Eq. (24) in [17], with the drop viscosity replaced with the effective viscosity, according to Eq. (9) in [14]). The numerical solutions gives $f_{el}^{(n)} = 17.31\text{ kHz}$, which is very close to the asymptotic solution.

4. Results and discussion

In all experiments, two sets of data were taken: with the particles crossing the laser beam when the ultrasound transducer was either on or off. When a particle passes through the test space, due to the Gaussian shape of the laser beam, the PMT records a relative peak with a quasi-Gaussian envelope, as exemplified in Fig. 3. The processing algorithm consists of straightforward steps. First, a threshold is set in order to select only high peaks that were

generated by particles crossing the laser beam and not from dust impurities in the water stream, or from detector/electronic noise. Then, boxcar smoothing can be applied to the signal, but it is used with caution because excessive averaging would discard ultrasound information. On the selected individual quasi-Gaussian peaks, the Fast Fourier Transform is performed.

Figure 4 displays the FFT of the optical signals from two cells, one with and one without ultrasound excitation. A broad feature is seen, centered around 20kHz, which is consistent with the theoretical calculation for Jurkat cell nuclei. The feature was not present for every cell during ultrasound excitation, but it *only* appeared when the US excitation was applied. This fact was attributed to occasional misalignments in time and space, between the cell position and the US pulse. The ultrasound pulses are generated every 100 μ s (i.e. 10kHz repetition rate) while a cell spends approximately 200 μ s in the laser beam. The ultrasound focus is on the order of 0.75 mm while the width of the jet that carries the particles is also around 0.75mm. The position of a cell inside the jet varies for each particle, and the jet exhibits some degree of position variation. It is thus possible that some cells are not hit with enough acoustic energy to undergo shape oscillations.

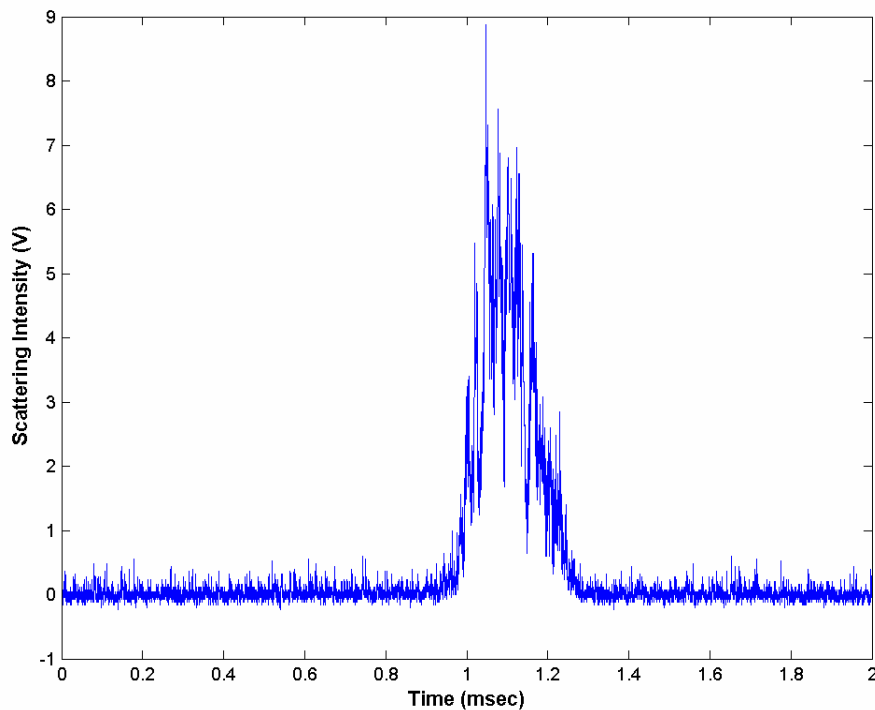


Fig. 3. Individual Peak.

For the same experiment, Fig. 5 displays the average of 75 FFTs of peaks taken with the ultrasound off (blue trace) and the average of 75 FFTs of peaks taken with the ultrasound on (red trace). The two curves separate only for a broad region around 20 kHz, which is the region of interest predicted by the theoretical calculation. The scale in Fig. 4 was double that of Fig. 5, to accommodate the enhanced signal at low frequency for that particular cell, relating to motion. Other individual cells had different low-frequency effects, and the average over many cells was zero difference at low frequency, as seen in Fig. 5.

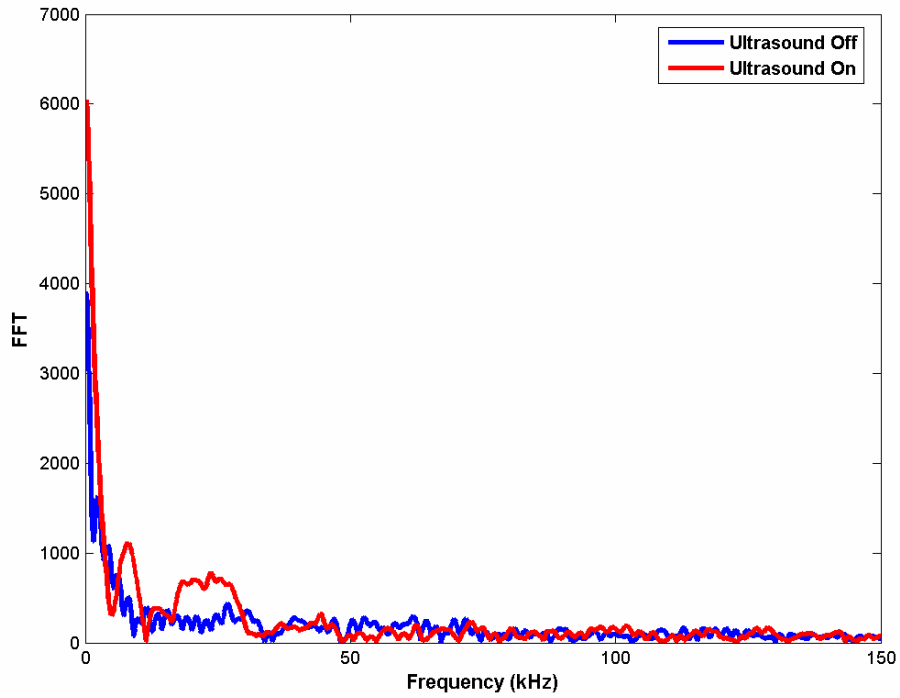


Fig. 4. FFT of one peak obtained with the ultrasound off and one peak obtained with the ultrasound on.

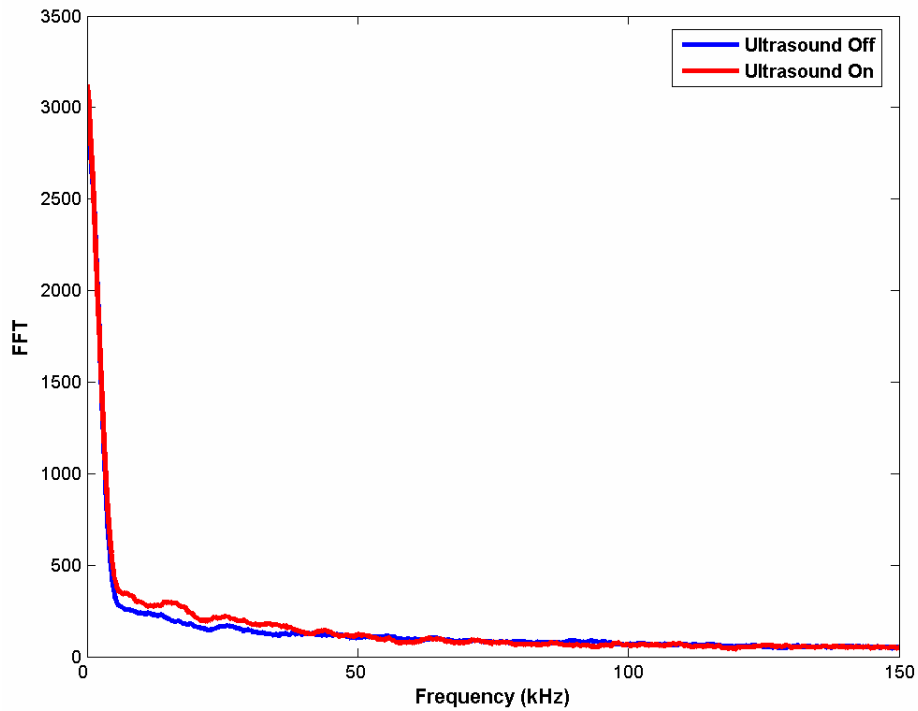


Fig. 5. Averaged FFTs of 75 peaks obtained with the ultrasound off and 75 peaks obtained with the ultrasound on.

Variations in the scattered intensities for individual cells are due, among other things, to the Gaussian profile of the laser beam and the fact that the cells do not all flow through the same region of the beam. Therefore, for the current stage of development of the instrument, a uniform size distribution of particles generates a distribution of amplitudes, which limits the accuracy of calibration and hinders attempts at accurate size extraction. Future instrument refinements should ameliorate the problem. The effect of shape oscillations, nonetheless, is repeatable and consistent with calculations. The unequal amplitudes problem has also, commonly, plagued flow cytometers. A number of solutions have been proposed by Hirleman (1980), which could be implemented for a flow-cytometer type of setup [18, 19].

Another future refinement of our system will be to investigate the resonant frequencies of cells using both s-polarized and p-polarized laser beams to obtain information about the cell's orientation and shape. Extensions of Mie theory have been applied to oblate and prolate spheroids and cylinders [9], and these will aid future refinements of data analysis. Of course, the hoped-for long-term utility of the reported method is to be able to distinguish among cells with different mechanical properties, related to different states of disease or other parameters. This report demonstrates that the signal is there, and future work will address the more subtle challenge of sensing differences in cell mechanics relating to underlying biological differences.

Acknowledgments

This work was supported in part by the NIH National Cancer Institute and by the Boston University Photonics Center. The authors gratefully acknowledge discussions with and equipment loaned by Prof. R.A. Roy. The authors also thank Dr. Ousama Aamar for his support while building the experimental setup and Christine Mulvey for help with the cell culture protocol.